

Supplementary Information

Probing the excited-state chemical shifts and exchange parameters by nitrogen-decoupled amide proton chemical exchange saturation transfer (HN^{dec} -CEST)

Qinglin Wu^a, Benjamin A. Fenton^a, Jessica L. Wojtaszek^{a,‡}, and Pei Zhou^{a*}

^a Department of Biochemistry, Duke University Medical Center, Durham, NC 27710, U.S.A

[‡] Current address: National Institute of Environmental Health Sciences, Research Triangle Park, NC 27709, U.S.A.

* Correspondence should be addressed to: peizhou@biochem.duke.edu

Materials and methods

Sample preparation

^{15}N -labeled and unlabeled ubiquitin and the FAAP20 UBZ domain were expressed and purified as previously described ¹. Concentrations of the purified protein samples were determined by the UV absorption at 280 nm. Two NMR samples were prepared. The first sample contains 1.33 mM of ^{15}N -labeled ubiquitin mixed with a 4.5% molar ratio of unlabeled FAAP20 UBZ. The second NMR sample contains 1.4 mM ^{15}N -labeled FAAP20 UBZ mixed with a 4.66% molar ratio of unlabeled ubiquitin. The NMR buffer contains 25 mM sodium phosphate (pH 7.0), 100 mM KCl, and 10% D_2O .

NMR spectroscopy

2D HN^{dec} -CEST experiments were recorded with a CEST mixing time of 95 ms at 25 °C on a Bruker 700 MHz spectrometer equipped with a room temperature $^1\text{H}/^{13}\text{C}/^{15}\text{N}$ triple-resonance probe for the sample of ^{15}N -labeled ubiquitin in complex with 4.5% unlabeled FAAP20 UBZ. Three datasets were collected at the experimentally determined ^1H B_1 fields of 14.8 Hz, 21.7 Hz, and 29.5 Hz, covering the chemical shift range from 7.1 ppm to 11.2 ppm with step sizes of 15 Hz, 22 Hz, and 30 Hz, respectively. The ^1H B_1 field inhomogeneity was determined to be 7.9% based on measured intensities of isolated signals following a series of hard pulses with flip angles from 0° to 780°. The signal loss of the longitudinal two-spin order $2\text{H}_z\text{N}_z$ caused by the nitrogen decoupling during the CEST period was determined by measurements with and without the WALTZ16 ^{15}N -decoupling scheme for a remote, off-resonance ^1H CEST frequency. NMR data were processed using NMRPipe ². The experimentally

measured chemical shift differences of five ubiquitin residues in the apo state and in the FAAP20 UBZ-bound state ¹ were used for comparison with those derived from the HN^{dec}-CEST measurements.

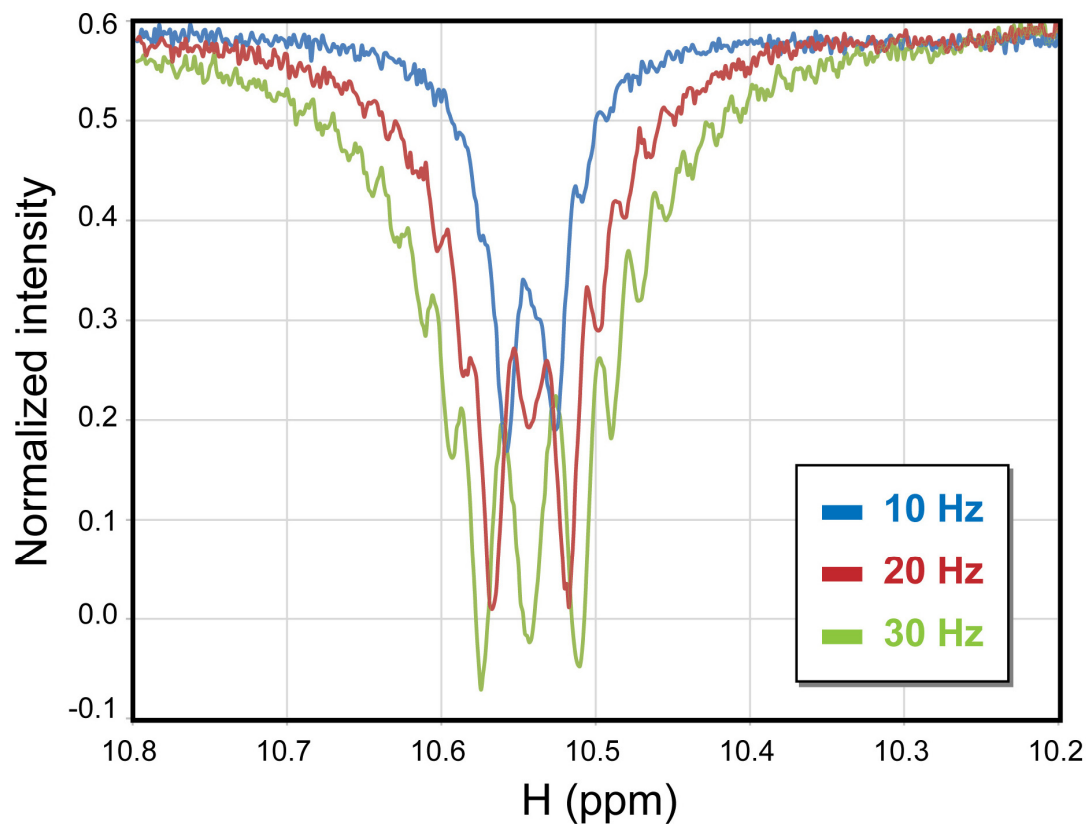
In order to demonstrate the reliability of the HN^{dec}-CEST experiment for measuring the exchange rate and excited state population from individual signals and from global fitting, we also carried out the ¹⁵N-CEST experiment ³ with a CEST mixing time of 300 ms. Three data sets were collected at the experimentally measured ¹⁵N B₁ fields of 16 Hz, 23 Hz, and 31 Hz, covering the chemical shift range from 94 ppm to 141.8 ppm with step sizes of 15 Hz, 22 Hz, and 30 Hz, respectively. NMR data were processed using NMRPipe ². The ¹⁵N B₁ field inhomogeneity was measured to be 6.7% based on hard nitrogen pulses with flip angles from 0° to 870°. As fitting of the ¹⁵N-CEST profiles using separate transverse relaxation rates for the excited state (R_2^E) and ground state (R_2^G) of individual residues did not improve the outcome (compare Tables S3 and S4), the final fitting was carried out by assuming equal transverse relaxation rates for the ground and excited states for individual residues (Table S3).

In order to illustrate the benefit of the HN^{dec}-CEST experiment in the situation of limited heteronuclear chemical shift difference between the ground and excited states, 1D HN^{dec}-CEST experiment and ¹⁵N-CEST experiments were carried out for the isolated HN signal of the tryptophan sidechain of W180 of ¹⁵N-labeled FAAP20 UBZ in the presence of 4.66% unlabeled ubiquitin. Three proton spinlocks of 14.3 Hz, 21.2 Hz and 28.9 Hz with a CEST mixing time of 95 ms were used for the 1D HN^{dec}-CEST experiment at step sizes of 10 Hz, 20 Hz, and 25 Hz, respectively. The proton B₁ field inhomogeneity and signal loss due to nitrogen decoupling during the CEST period were experimentally determined to be 7.3% and 4%, respectively. Three nitrogen spinlocks of 15.9 Hz, 23.1 Hz, and 31.4 Hz with a CEST mixing time of 400 ms were

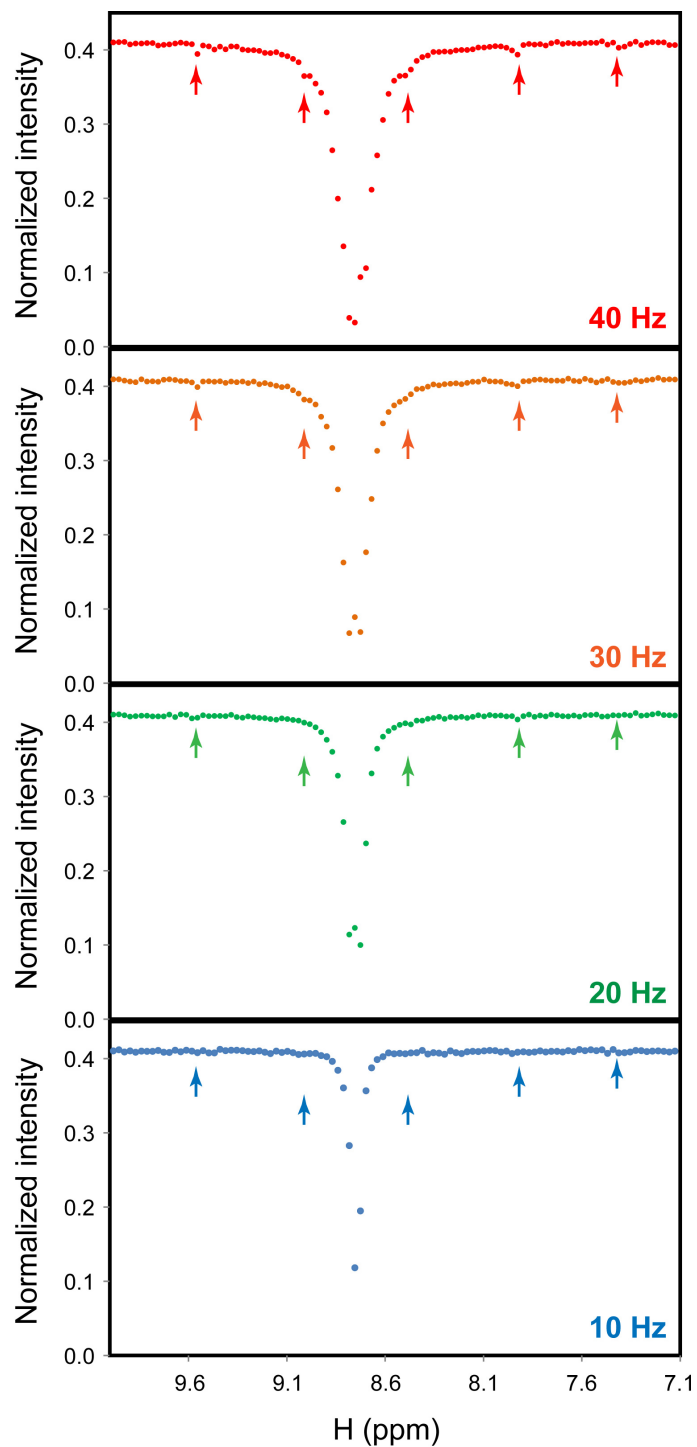
used for the 1D ^{15}N -CEST experiment at step sizes of 15 Hz, 22 Hz, and 30 Hz, respectively.

The nitrogen B_1 field inhomogeneity (6.7%) was determined experimentally.

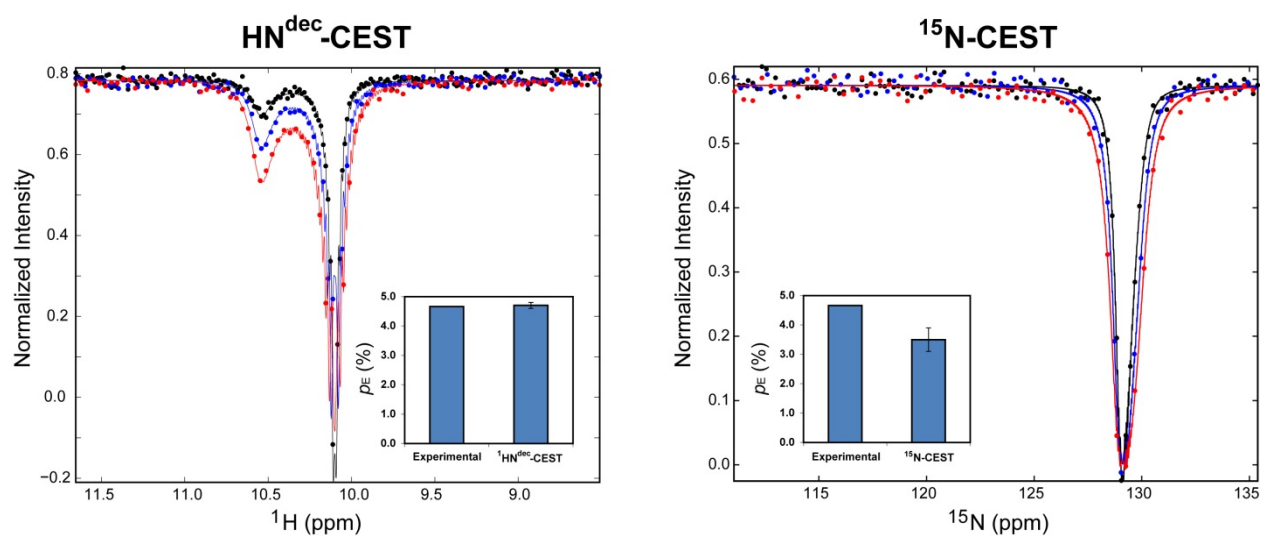
Supplementary Figures



Supplementary Figure S1. Examples of the oscillating HN^{dec} -CEST profiles due to the short CEST transfer time. The CEST profiles were collected using ^{15}N -labeled protein G B1 domain ^{4,5} by monitoring the isolated tryptophan sidechain signal of W43 at the step size of 1 Hz, with proton B_1 fields at 10 Hz (blue), 20 Hz (maroon) and 30 Hz (light green).



Supplementary Figure S2. Decoupling sidebands in the HN^{dec} -CEST experiment. The locations of decoupling sidebands at the 40 Hz spinlock field are marked by red arrows. Diminishing decoupling sidebands are observed at lower spinlocks fields (30 Hz, 20 Hz and 10 Hz).



Supplementary Figure S3. The HN^{dec} -CEST experiment enables more robust extraction of the exchange parameters, such as the excited state population p_E , than the ^{15}N -CEST experiment in the situation of limited heteronuclear chemical shift difference between the ground and excited states. The HN^{dec} -CEST and ^{15}N -CEST profiles were collected for the sidechain of the disordered C-terminal tryptophan residue (W180) of FAAP20 UBZ, which folds around I44 of ubiquitin in the FAAP20 UBZ-ubiquitin complex. Proton spinlock frequencies of 14.3 Hz (black), 21.2 Hz (blue) and 28.9 Hz (red) were used for the HN^{dec} -CEST experiment and nitrogen spinlock frequencies of 15.9 Hz (black), 23.1 Hz (blue) and 31.4 Hz (red) were used for the ^{15}N -CEST experiment. The populations of the excited state (the FAAP20 UBZ-ubiquitin complex) determined from UV measurements (experimental) and from HN^{dec} -CEST and ^{15}N -CEST experiments are shown as bar graphs.

Supplementary Tables

Table S1. Fitting results of the HN^{dec}-CEST experiment ($R_2^E = R_2^G$)

Residue	$R_1^{G/E}$ (s ⁻¹)	$R_2^{G/E}$ (s ⁻¹)	$\Delta\omega$ (ppm)	k_{ex} (s ⁻¹)	p _E (%)	drift (ppm)	χ^2
G47	8.36±0.01	15.9±1.0	1.710±0.003	319±18	4.4±0.1	-0.0019±0.0002	0.43
K48	5.52±0.01	11.4±0.9	-0.212±0.004	361±24	4.2±0.1	-0.0027±0.0002	0.58
Q49	8.09±0.01	12.8±0.8	-0.494±0.003	342±14	4.7±0.1	-0.0026±0.0002	0.70
V70	7.93±0.01	18.1±0.6	0.224±0.002	298±13	4.5±0.1	-0.0016±0.0002	0.26
L71	6.79±0.01	9.8±0.8	0.285±0.003	370±15	4.9±0.1	0.0022±0.0002	0.78
Mean				338±30	4.5±0.3		0.55±0.21
Global				343±7	4.52±0.04		0.54

Table S2. Fitting results of the HN^{dec}-CEST experiment (separate R_2^E and R_2^G)

Residue	$R_1^{G/E}$ (s ⁻¹)	R_2^G (s ⁻¹)	R_2^E (s ⁻¹)	$\Delta\omega$ (ppm)	k_{ex} (s ⁻¹)	p _E (%)	drift (ppm)	χ^2
G47	8.36±0.01	18.8±2.0	96±44	1.708±0.003	239±51	4.7±0.2	-0.0020±0.0002	0.43
K48	5.52±0.01	11.5±0.9	32±36	-0.209±0.007	347±38	4.3±0.3	-0.0027±0.0003	0.59
Q49	8.09±0.01	12.8±1.1	13±34	-0.494±0.004	342±29	4.7±0.2	-0.0026±0.0002	0.71
V70	7.92±0.01	18.4±0.6	50±20	0.220±0.004	272±21	4.7±0.2	-0.0017±0.0002	0.26
L71	6.79±0.01	9.8±0.9	10±28	0.285±0.004	370±26	4.9±0.2	0.0022±0.0002	0.78
Mean					314±56	4.7±0.2		0.55±0.21

Table S3. Fitting parameters of the ¹⁵N-CEST experiment ($R_2^E = R_2^G$)

Residue	$R_1^{G/E}$ (s ⁻¹)	$R_2^{G/E}$ (s ⁻¹)	$\Delta\omega$ (ppm)	k_{ex} (s ⁻¹)	p _E (%)	drift (ppm)	χ^2
G47	2.915±0.002	7.1±0.4	1.98±0.01	330±8	4.95±0.07	0.014±0.005	0.31
K48	2.299±0.003	9.0±0.6	-2.79±0.01	338±10	4.74±0.07	0.015±0.007	1.07
Q49	2.762±0.002	7.3±0.5	-3.64±0.01	332±7	4.82±0.05	-0.012±0.006	0.93
V70	2.198±0.001	8.3±0.3	2.29±0.01	364±6	4.80±0.05	0.005±0.004	0.37
L71	2.144±0.001	6.3±0.3	3.07±0.01	345±4	4.93±0.03	0.005±0.003	0.41
Mean				342±14	4.8±0.1		0.62±0.35
Global				342±3	4.84±0.02		0.62

Table S4. Fitting results of the ¹⁵N-CEST experiment (separate R_2^E and R_2^G)

Residue	$R_1^{G/E}$ (s ⁻¹)	R_2^G (s ⁻¹)	R_2^E (s ⁻¹)	$\Delta\omega$ (ppm)	k_{ex} (s ⁻¹)	p _E (%)	drift (ppm)	χ^2
G47	2.914±0.002	7.0±0.4	20±8	1.96±0.02	318±11	5.06±0.10	0.015±0.005	0.30
K48	2.298±0.003	9.1±0.6	16±13	-2.77±0.02	331±15	4.78±0.09	0.016±0.007	1.07
Q49	2.762±0.003	7.3±0.5	7±12	-3.64±0.02	332±13	4.82±0.07	-0.012±0.006	0.93
V70	2.197±0.001	8.4±0.3	32±7	2.25±0.01	341±9	4.96±0.07	0.006±0.004	0.36
L71	2.144±0.001	6.3±0.3	6±6	3.07±0.01	345±7	4.93±0.04	0.005±0.003	0.41
Mean					333±11	4.9±0.1		0.61±0.36

Table S5. Fitting results of the $^1\text{HN}^{\text{dec}}$ -CEST and ^{15}N -CEST experiment ($R_2^E = R_2^G$) for the C-terminal tryptophan sidechain of FAAP20 UBZ in the presence of 4.66% ubiquitin

Data Type	$R_1^{G/E}$ (s^{-1})	R_2^G (s^{-1})	$\Delta\omega$ (ppm)	k_{ex} (s^{-1})	p_E (%)	drift (ppm)	χ^2
HN^{dec} -CEST	2.134±0.007	3.4±0.6	0.451±0.002	279±10	4.7±0.1	-0.006±0.000	0.77
^{15}N -CEST	1.316±0.003	1.7±0.3	-0.699±0.024	282±28	3.5±0.4	0.025±0.003	1.15
Sample					4.66		

References

1. J. L. Wojtaszek, S. Wang, H. Kim, Q. Wu, A. D. D'Andrea and P. Zhou, *Nucleic Acids Res.*, 2014, **42**, 13997-14005.
2. F. Delaglio, S. Grzesiek, G. W. Vuister, G. Zhu, J. Pfeifer and A. Bax, *J. Biomol. NMR*, 1995, **6**, 277-293.
3. P. Vallurupalli, G. Bouvignies and L. E. Kay, *J. Am. Chem. Soc.*, 2012, **134**, 8148-8161.
4. P. Zhou, A. A. Lugovskoy and G. Wagner, *J. Biomol. NMR*, 2001, **20**, 11-14.
5. P. Zhou and G. Wagner, *J. Biomol. NMR*, 2010, **46**, 23-31.